BULLETIN OF THE EARTHQUAKE
RESEARCH INSTITUTE
Vol. 46 (1968), pp. 667-686

30. *Some Features of Strong Underground Earthquake Motions Computed from Observed Surface Records.*

By Shizuyo YOSHIZAWA, Teiji TANAKA
and Kiyoshi KANAI,

Earthquake Research Institute.

(Read Nov. 28, 1967.—Received March 30, 1968.)

1. Introduction

The strong-motion seismograms obtained to date in Japan and the U.S.A. have been used extensively for the dynamic design and analysis of important structures. However, two factors limit the validity of direct application of the seismograms as well as the derived response spectra. First, most of the seismograms used for these analyses were obtained on or very near the ground surface, consequently recorded ground motions are modified by surficial soil layers. Second, large heavy structures are founded generally on a competent subsurface formation capable of supporting them.

Thus, seismograms recorded at one site are not always adequate for the design and analysis of structures at other sites having different subsoil conditions or for unusual structures whose foundations are relatively deep.

To overcome these limitations, two methods have been developed to obtain the waveforms of strong earthquake motions under the ground.

One method is by subsurface earthquake observation to get direct information of strong earthquake motions that are almost undisturbed by the surficial soil layers. This method has been used recently in Japan as well as in the U.S.A. However, there is little hope of obtaining a sufficient quantity of records of strong earthquakes under the ground in the near future because of the small number of observation stations.

The second method is to estimate the waveforms of underground motions on the basis of those at the surface by application of the theory

of multiple reflections of waves in the layered ground[1)-4)].

This paper is concerned with the second method and presents results of computation for the waveforms of underground motion, in which most of the predominant surficial vibrations at the observation site have been eliminated, on the basis of strong-motion seismograms recorded in Japan and the U.S.A. The derived response spectra of the single-degree-of-freedom system from both the original and computed waveforms are also presented for comparison of their effects on structures.

2. Waveform of earthquake motions at depth corresponding to foundation bed of a structure

The formation regarded as a bearing base for the foundations of large heavy structures usually corresponds dynamically to the second layer of the stratified ground, which lies within a few tens of meters below the surface. Therefore, earthquake motion on the second layer of the ground is more significant than that on the surface from the standpoint of earthquake engineering.

The relation between the waveforms of earthquake motions at the ground surface, $U_S(t)$, and those at a point in the first layer of the ground, $U_1(t)$, has been given by two of the authors, and is based on the concept of multiple reflection of waves in an elastic layer, as follows[5)],

$$U_1(t-\tau)=\frac{1}{2}[U_S(t)+U_S(t-2\tau)] \qquad (1)$$

where, τ is z/V_1 and, z and V_1 respectively are the depth in question from the surface and the propagation velocity of waves in the layer. For the lower boundary of the layer, τ_1 is equal to H_1/V_1, in which H_1 is the thickness of the layer, and then the value of τ_1 may be estimated

1) K. KANAI and S. YOSHIZAWA, "Some New Problems of Seismic Vibrations of a Structure, Part 1," *Bull. Earthq. Res. Inst.*, **41** (1963), 825-833.

2) E. SHIMA, "Modifications of Seismic Waves in Superficial Soil Layers as Verified by Comparative Observations on and beneath the Surface," *Bull. Earthq. Res. Inst.*, **40** (1962), 187-259.

3) H. KAWASUMI and E. SHIMA, "Standard Strong Earthquake Motion for the Use in Antiseismic Designing," *Proc. Japan National Symp. Earthq. Engg.*, (1962) 13 (in Japanese).

4) H. KOBAYASHI and H. KAGAMI, "Study of Motions at Bed Rock Assumed from Strong Earthquake Motions," *Trans. Arch. Inst. Japan*, Extra (1967), 163 (in Japanese).

5) *loc. cit.*, 1).

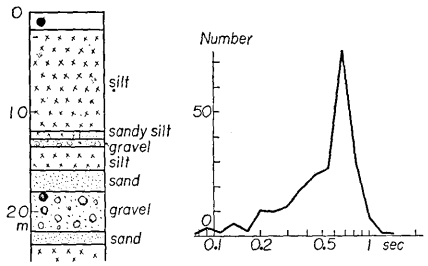

Fig. 1. Subsoil conditions and the period distributions of microtremors of the ground at Marunouchi, Tokyo.

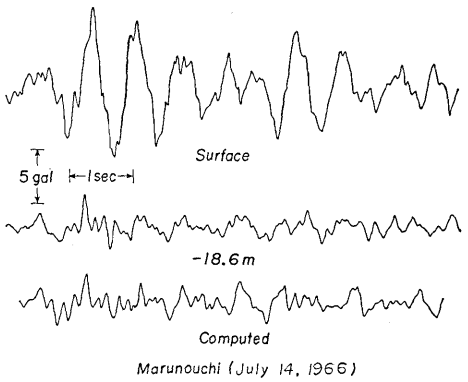

Fig. 2. Seismograms obtained on the surface and at 18.6 m depth and the computed waveform for the observation site, Marunouchi, Tokyo.

from the predominant period of earthquake motions or microtremors observed on the surface, T_G, by using the relation, $T_G=4\tau_1$. Good applicability of this simple equation to actual seismograms has been proved by comparison of earthquakes observed underground and on the surface[6].

A result of application of this method to the seismograms recorded at Marunouchi, Tokyo is given, as an example. Subsoil conditions were determined by boring at the observation site (see Fig. 1). The thickness of the alluvial and diluvial deposits above the Tokyo gravel bed is 18.6 m in that site. This gravel bed is an important formation since it is the most reliable bearing base for large structures in the lowland area of Tokyo.

Fig. 2 presents seismograms of a medium earthquake recorded both on the surface and in the Tokyo gravel bed by bore hole seismometers and the resulting computed waveform. In this computation, the value of 0.7 sec was adopted as the predominant period of ground, determined from the result of microtremors observation on the surface as shown in Fig. 1. This example not only exhibits how the weak layer near the surface plays an important role in the modification of seismic waves but also shows that the method is valuable in gaining information of the earthquake motion under the ground.

6) K. KANAI et al., "Comparative Studies of Earthquake Motions on the Ground and Underground. II," *Bull. Earthq. Res. Inst.*, **44** (1966), 609-643.

Table 1. Strong earthquake records treated in the study.

No.	Station	Date	Orientation	Max. Accel. (gal)	$4\tau_1$	Remarks
1	Kushiro	Apr. 23, 1962	N159E	385	0.30	C
			N69E	240		
2	Akita	June 16, 1964	NS	90	0.30	C
			EW	80		
3	Hoshina	Apr. 5, 1966	NS	220	0.10	D
			EW	420		
4	Wakaho	Apr. 5, 1966	NS	260	0.40	D
			EW	250		
5	El Centro	Dec. 30, 1934	NS	260	0.23	A
			EW	180		
6		May 18, 1940	NS	330	0.23, 0.50	B
			EW	230		
7	Taft	July 21, 1952	NS	180	0.29	B
			EW	150		
8	Vernon	Mar. 10, 1933	N08E	130	0.40	A
			N98E	190		
9		Oct. 2, 1933	N08E	90	0.40	A
			N98E	120		
10	Santa Barbara	June 30, 1941	N42E	230	0.26	A
			N132E	240		

A: J. L. Alford, G. W. Housner and R. R. Martel, "Spectrum Analysis of Strong-Motion Earthquakes," lst Tech. Rep. Office Nav. Res., Contr. No. 6onr-244, Task Order 25, Project Design, NR-081-091-(1951).

B: K. Muto et al., "Digital Values for Analog Computation by SERAC," Preprint of SERAC Report No. 6, (1964).

C: Strong-Motion Earthq. Obs. Comm., "Strong-Motion Earthquake Records in Japan," Vol. 2 (1965).

D: Strong Earthq. Motion Obs. Center, ERI, "Strong Earthquake Motion Records in Matsushiro Earthquake Swarm Area," (1967).

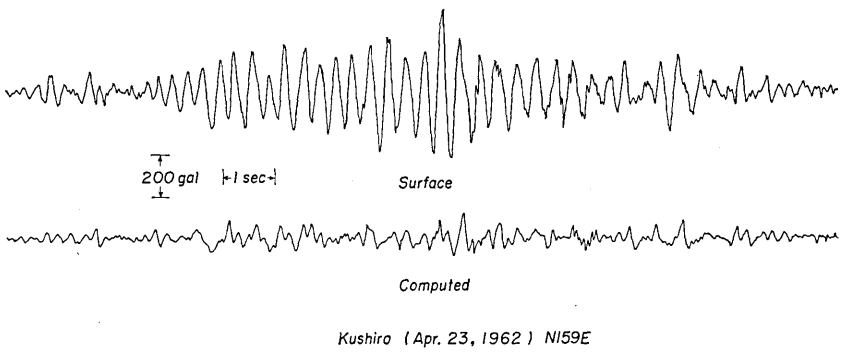

Fig. 3. Seismogram obtained on the surface and the computed waveform for the Kushiro station.

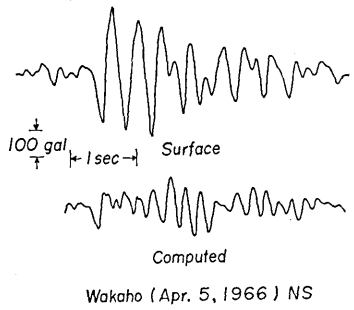

Fig. 4. Seismogram obtained on the surface and the computed waveform for the Wakaho station.

Numerical computations by the above-mentioned method were made for 20 strong earthquake records obtained at 8 stations in Japan and the U. S. A. Some of the data relating to these records are listed in Table 1. The original acceleration records in both analogue and digital forms were used in the study, and their sources are indicated in Table 1. For the digital records of El Centro (1940) and Taft (1952) consisting of only maxima and minima, given by G. V. Berg, cosine-curve interpolation method was applied. As for the analogue records, the digitization of amplitudes at about 1/100 sec intervals was performed by using the SMAC Digitizer.

Figs. 3 and 4 show the recorded and computed waveforms for the Hiroo-oki earthquake of 1962 (N159E-component) observed at Kushiro Meteorological Observatory, and a strong earthquake associated with the Matsushiro earthquake swarm in 1966 (NS-component) obtained at the Wakaho Town Office. The value of $4\tau_1$ adopted in the computation is 0.30 sec for Kushiro and 0.40 sec for Wakaho, as estimated from the results of microtremors observations at the respective sites[7),8)]. Figs. 3 and

7) K. KANAI et al., "An Empirical Formula for the Spectrum of Strong Earthquake Motions. II," *Bull. Earthq. Res. Inst.*, **41** (1963), 261-270.

8) K. KANAI et al., "Observation of Microtremors. XI. (Matsushiro Earthquake Swarm Area)," *Bull. Earthq. Res. Inst.*, **44** (1966), 1297-1333.

4 indicate a great difference between the original and computed waveforms. The important point, however, is not the magnitudes of maximum acceleration but the waveform itself, on which the response characteristics of a structure depend.

Using data from Table 1, acceleration spectra of the linear single mass system of 20 different records (10 in 2 components each) and the derived waveforms are presented in Fig. 8 for 5% and 10% of critical damping. The analyses utilized the SERAC analogue computer at the University of Tokyo. Among the spectra for the observed records, those of Akita (1964), El Centro (1940) and Taft (1952) are from the SERAC report[9].

The values of $4\tau_1$ used for each observation site are indicated in the sixth column of Table 1. For the El Centro record of the Imperial Valley earthquake of 1940, two different values of $4\tau_1$ were adopted because two distinct periods of about 0.2 sec and 0.5 sec appear on the record. Fig. 8 shows that the shapes of response curves for the computed waveforms exhibit a tendency to flatten as a whole, and the amplitudes of response at the neighborhood of the predominant period of the ground diminish to 1/2–1/5 compared with those of the original records at the surface.

To aid in comparison, the results of Fourier analyses of the recorded and computed waveforms are shown in Fig. 11.

3. The case of multi-layered ground

Where the thickness, density, and velocity of wave propagation for each layer of stratified ground are known, the waveform of earthquake motions at any depth can be deduced from the waveform on the surface by a method based on the multiple reflection theory of elastic waves[10] (summarized in the Appendix). However, this basic information is not presently available for most sites of strong-motion seismograph stations, especially those in Japan.

In this section of the paper, the method is applied to some strong-motion seismograms obtained in the U. S. A. The results of computation of the waveforms at every boundary of the layers, as well as those of the incident waves from bedrock to the lowest layer for the strong

9) Strong Earthq. Response Analysis Committee, "Non-linear Response Analysis of Tall Building to Strong Earthquake and its Application to Dynamic Design," *SERAC Report* No. 4 (1964), No. 6 (1966).

10) *loc. cit.*, 4).

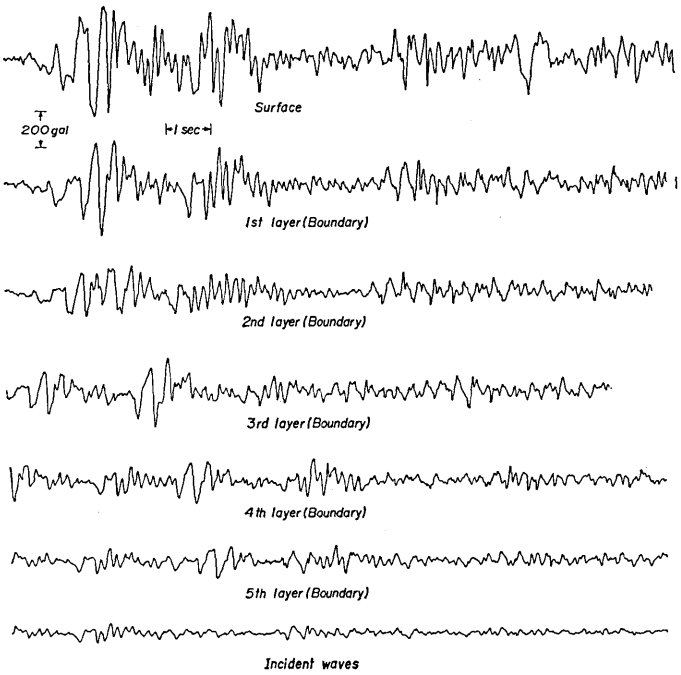

Fig. 5. Seismogram obtained on the surface, and the computed waveforms at each boundary of the layers and the incident waves for the El Centro station (May 18, 1940, NS).

shocks at El Centro in 1940 and Taft in 1952, are illustrated in Figs. 5 and 6. The *S*-velocity and density distributions with depth for both sites are shown in Fig. 7. These data are from U.C.L.A. Engineering Department reports on the site characteristics of Southern California strong motion earthquake stations[11]. The acceleration spectra for these observed and computed waveforms are plotted in Figs. 9 and 10. An important assumption made in the method is that the most significant part of earthquake motions on the ground surface is caused by transversal waves.

Although all results computed for each boundary of the layers and for the incident waves are given, the results for the uppermost layer

11) C. M. DUKE and D. J. LEEDS, "Site Characteristics of Southern California Strong-Motion Earthquake Stations," *Report of Dept. Engg. Univ. Calif. L. A.*, 62-55, (1962).
R. B. MATTHIESEN et al., "Site Characteristics of Southern California Strong-Motion Earthquake Stations, Part Two," *ditto*, 64-15, (1964).

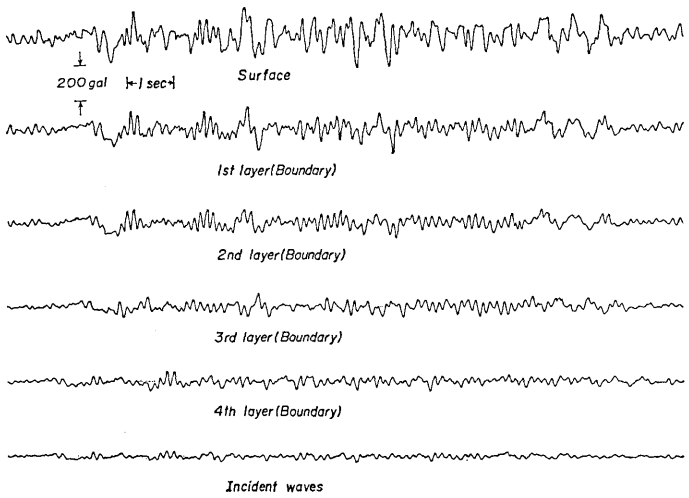

Fig. 6. Seismogram obtained on the surface, and the computed waveforms at each boundary of the layers and the incident waves for the Taft station (July 21, 1952, NS).

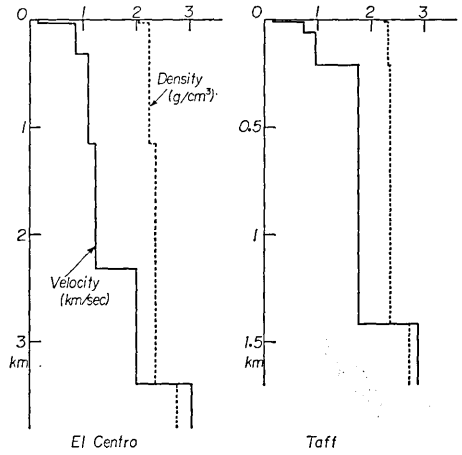

Fig. 7. S-velocity and density distributions with depth for the sites El Centro and Taft.

appear most significant from an engineering viewpoint. It should be added that the reliability of these computed results depends largely on the accuracy of the data of subsoil composition and physical properties for a given site.

4. Concluding remarks

In order to investigate the features of strong earthquake motions underground, the waveforms of the motions at each boundary of the layers, mainly of the first layer, of the stratified ground were computed from strong-motion seismograph records obtained in Japan and the U.S.A. The computation method used is based on the multiple reflection theory of elastic waves. The linear responses of the single-degree-of-freedom system for both the recorded and computed waveforms were also evaluated to estimate their effects on structures.

As might be expected, results of the computation show that there is much and significant difference between the waveforms of earthquake motions under the ground and on the surface with respect to the dynamic response of structures. This would suggest that for the earthquake response analysis of large heavy structures, based a considerable depth underground, the direct use of strong-motion seismograms observed at the surface is not always suitable.

5. Acknowledgments

The authors express their sincere thanks to Prof. H. Umemura and Prof. Y. Satô for use of the analogue computer SERAC and the computer program in Fourier analysis, respectively.

The cooperation of Mr. T. Nishikawa, a graduate student of the University of Tokyo, in the computation of the response spectra is also gratefully acknowledged.

The computation in this study was carried out through the courtesy of the Computer Center of the University of Tokyo.

Appendix

Let F, G and u be the waves propagating normally to layers upward and downward, and the resulting displacement in the layers. The origin of the waves are taken at the upper boundary of each layer, from which z is measured downward. The layers are numbered from top to bottom, so the quantities related to the uppermost layer and the bottom layer are denoted by the suffixes 1 and n, and the semi-infinite bedrock $n+1$.

Then, assuming the viscosity of the medium is negligibly small, the displacement of the i^{th} layer at time, t, may be expressed by

$$u_i(t)=F_i\left(t+\frac{z_i}{V_i}\right)+G_i\left(t-\frac{z_i}{V_i}\right), \tag{1}$$

where V_i is the propagation velocity of the waves in that layer.

Accordingly, the displacements at the upper and the lower boundaries of the layer are written respectively as

$$u_{i,z=0}(t)=F_i(t)+G_i(t), \tag{2}$$

and

$$u_{i,z=H_i}(t)=F_i(t+\tau_i)+G_i(t-\tau_i), \tag{3}$$

where τ_i is H_i/V_i and H_i is thickness of the layer.

Taking the time delay of the upward and downward waves of the i^{th} and the $i+1^{\text{th}}$ layer to arrive at the boundary into consideration, we have the following relations between them for the upper boundary of the layer $i+1$:

$$F_{i+1}(t)=\frac{1}{\gamma_i}F_i(t+\tau_{i+1})-\frac{\beta'_i}{\gamma_i}G_i(t-\tau_i), \tag{4}$$

$$G_{i+1}(t)=\beta_i F_{i+1}(t)+\gamma'_i G_i(t-\tau_i), \tag{5}$$

where

$$\left.\begin{aligned}&\gamma_i=2/(1+\alpha_i), \quad \beta_i=(1-\alpha_i)/(1+\alpha_i),\\ &\gamma'_i=2\alpha_i/(1+\alpha_i), \quad \beta'_i=(\alpha_i-1)/(\alpha_i+1),\end{aligned}\right\} \tag{6}$$

$$\left.\begin{aligned}&\tau_i=H_i/V_i, \quad \tau_{i+1}=H_{i+1}/V_{i+1},\\ &\alpha_i=\rho_i V_i/\rho_{i+1}V_{i+1}\end{aligned}\right\} \tag{7}$$

in which ρ is the density of the medium.

Equations (4) and (5) mean that the upward and downward waves of a layer can be determined from those of the upper layer. Therefore, we can obtain in turn $F_2(t)$, $G_2(t)$ ..... $F_n(t)$, $G_n(t)$, starting with the condition at the surface:

$$F_1(t)=G_1(t)=\frac{1}{2}u_0(t), \tag{8}$$

in which u_0 is the displacement at the surface of the ground.

The incident waves from the bedrock to the bottom layer (n^{th} layer), v, can also be obtained by merely substituting v for F_{n+1}.

These equations were programmed for computation by a digital computer. In the program, the values of F, G, u and v at time shifted by τ to the original values given at a definite time interval are evaluated by the Lagrange five points interpolation method.

The direct expressions of the displacements at each of the lower boundaries of the layers and those of the incident waves to the bottom layer can easily be obtained. The results for one-, two-, and three-layered ground are as follows:

$$
\left.\begin{aligned}
u_{1,\,z=H_1}(t) &= \frac{1}{2}\{u_0(t+\tau_1)+u_0(t-\tau_1)\}\\
u_{2,\,z=H_2}(t) &= \frac{1}{2\gamma_1}\{u_0(t+\tau_1+\tau_2)+\beta_1 u_0(t-\tau_1+\tau_2)\\
&\quad +\beta_1 u_0(t+\tau_1-\tau_2)+u_0(t-\tau_1-\tau_2)\}\\
u_{3,\,z=H_3}(t) &= \frac{1}{2\gamma_1\gamma_2}\{u_0(t+\tau_1+\tau_2+\tau_3)+\beta_1 u_0(t-\tau_1+\tau_2+\tau_3)\\
&\quad +\beta_1\beta_2 u_0(t+\tau_1-\tau_2+\tau_3)+\beta_2 u_0(t-\tau_1-\tau_2+\tau_3)\\
&\quad +\beta_2 u_0(t+\tau_1+\tau_2-\tau_3)+\beta_1\beta_2 u_0(t-\tau_1+\tau_2-\tau_3)\\
&\quad +\beta_1 u_0(t+\tau_1-\tau_2-\tau_3)+u_0(t-\tau_1-\tau_2-\tau_3)\}
\end{aligned}\right\} \tag{10}
$$

$$
\left.\begin{aligned}
v_1(t) &= \frac{1}{2\gamma_1}\{u_0(t+\tau_1)+\beta_1 u_0(t-\tau_1)\}\\
v_2(t) &= \frac{1}{2\gamma_1\gamma_2}\{u_0(t+\tau_1+\tau_2)+\beta_1 u_0(t-\tau_1+\tau_2)\\
&\quad +\beta_1\beta_2 u_0(t+\tau_1-\tau_2)+\beta_2 u_0(t-\tau_1-\tau_2)\}\\
v_3(t) &= \frac{1}{2\gamma_1\gamma_2\gamma_3}\{u_0(t+\tau_1+\tau_2+\tau_3)+\beta_1 u_0(t-\tau_1+\tau_2+\tau_3)\\
&\quad +\beta_1\beta_2 u_0(t+\tau_1-\tau_2+\tau_3)+\beta_2 u_0(t-\tau_1-\tau_2+\tau_3)\\
&\quad +\beta_2\beta_3 u_0(t+\tau_1+\tau_2-\tau_3)+\beta_1\beta_2\beta_3 u_0(t-\tau_1+\tau_2-\tau_3)\\
&\quad +\beta_1\beta_3 u_0(t+\tau_1-\tau_2-\tau_3)+\beta_3 u_0(t-\tau_1-\tau_2-\tau_3)\}\ .
\end{aligned}\right\} \tag{11}
$$

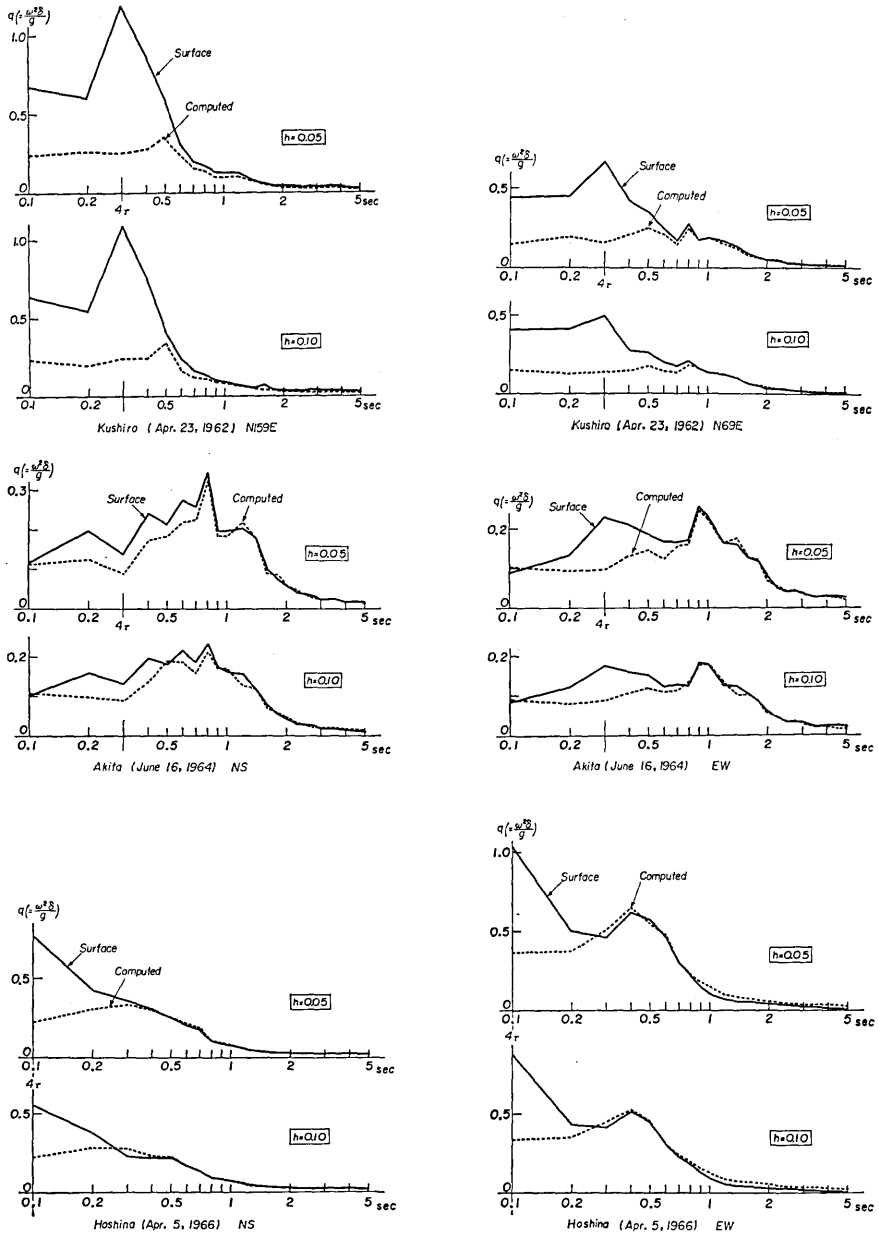

Fig. 8-a. Acceleration spectra for observed and computed waveforms.

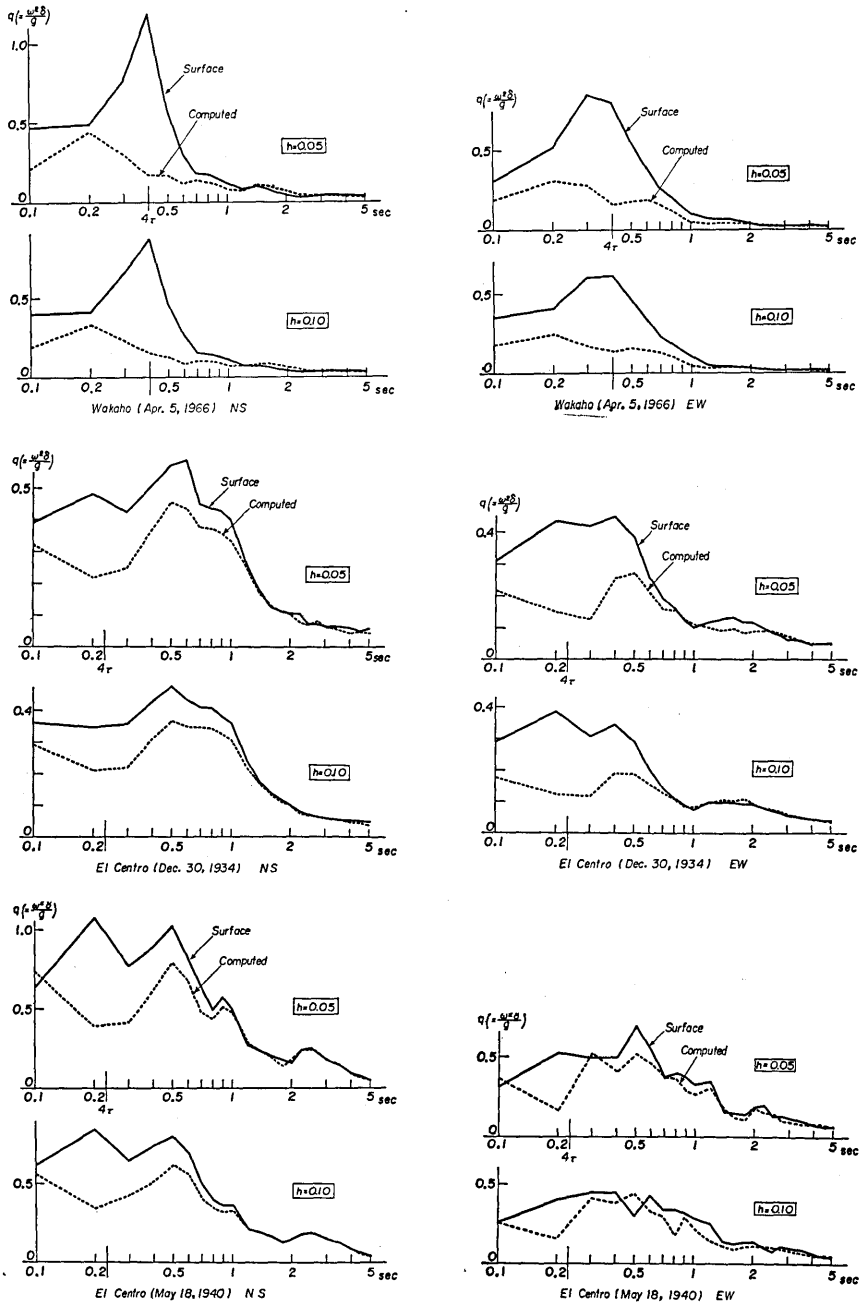

Fig. 8-b. Acceleration spectra for observed and computed waveforms.

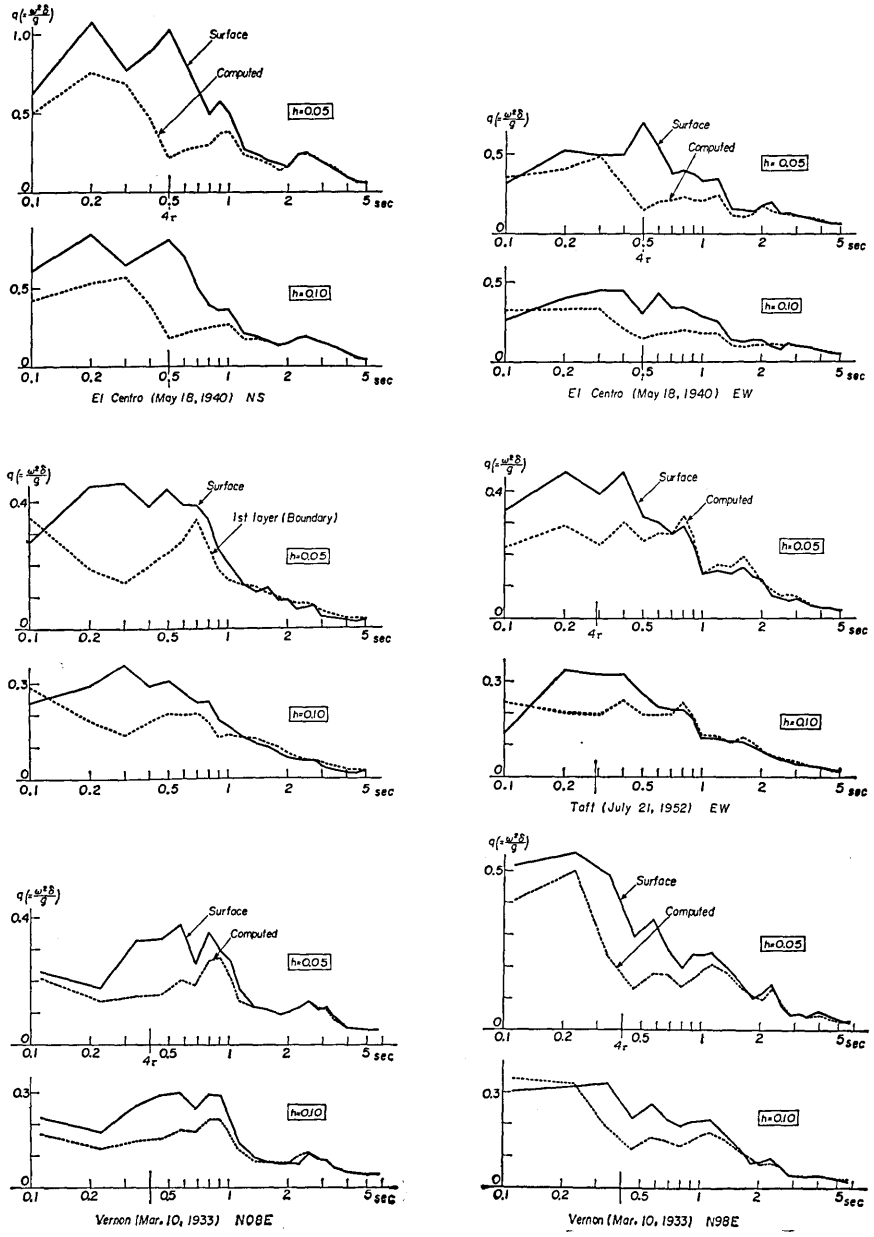

Fig. 8-c. Acceleration spectra for observed and computed waveforms.

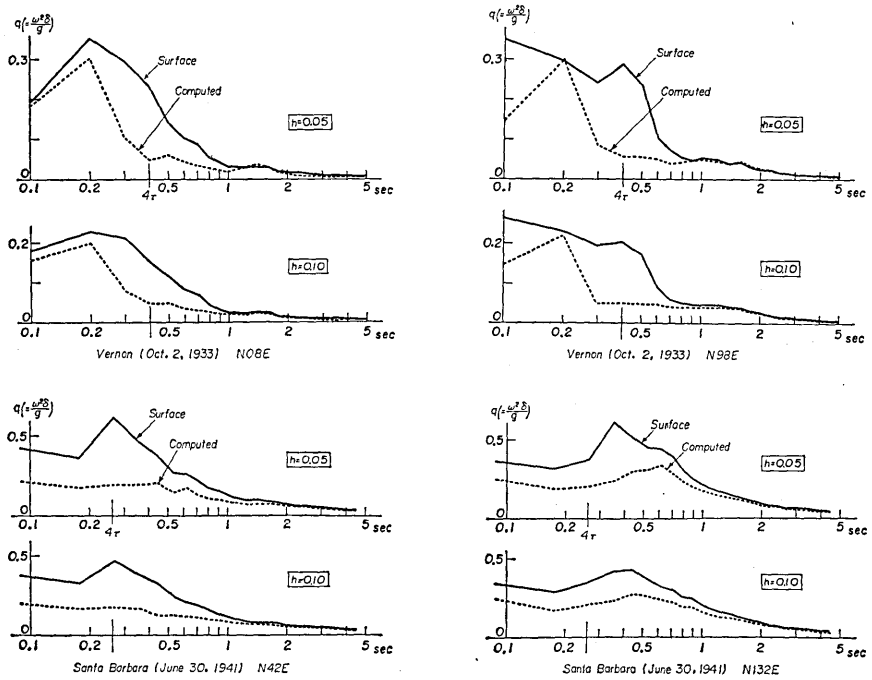

Fig. 8-d. Acceleration spectra for observed and computed waveforms.

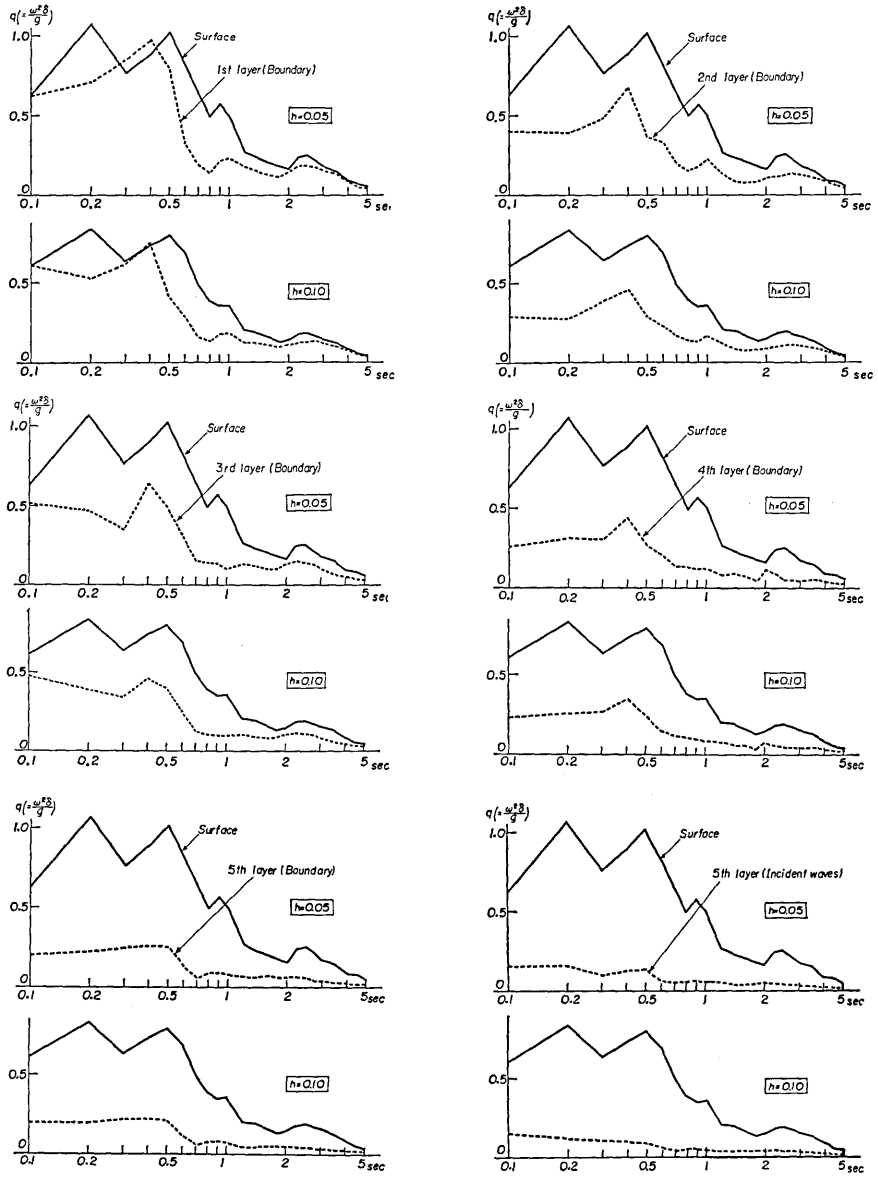

Fig. 9. Acceleration spectra for observed and computed waveforms at each boundary of the layers and the incident waves (El Centro, 1940).

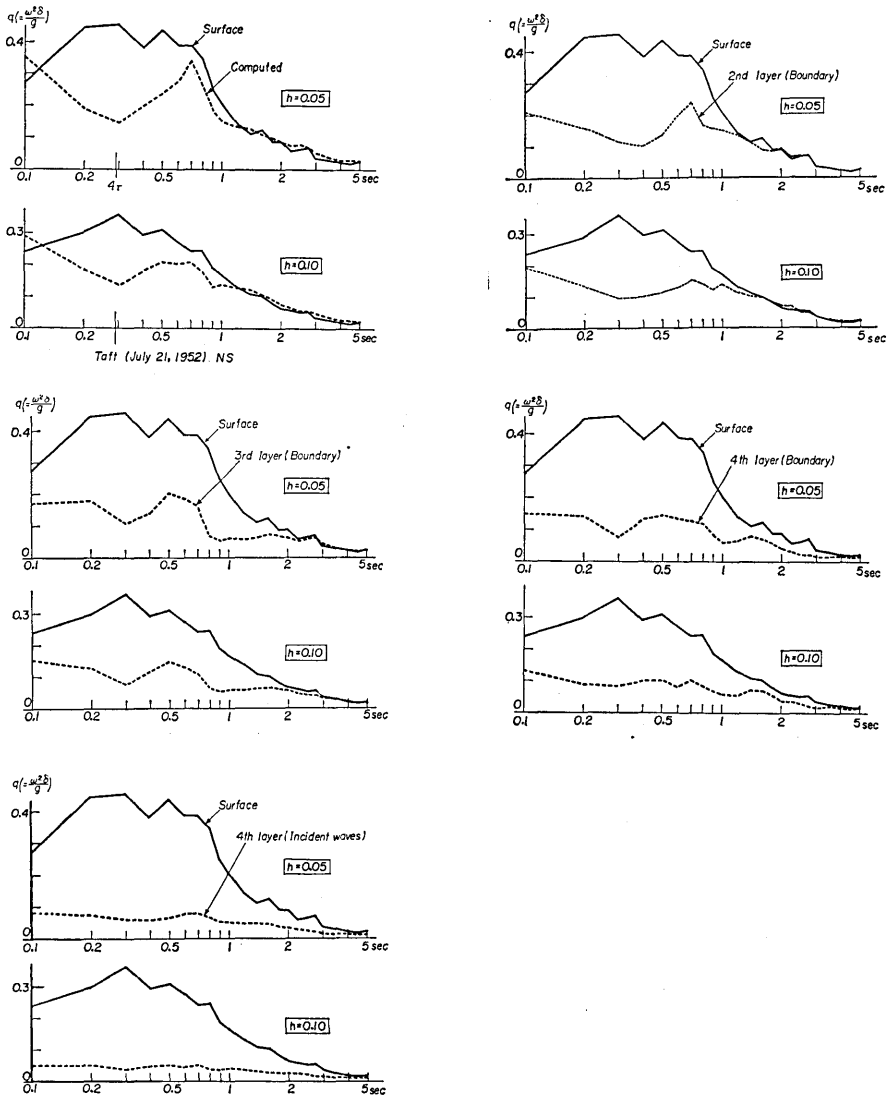

Fig. 10. Acceleration spectra for observed and computed waveforms at each boundary of the layers and the incident waves (Taft, 1952).

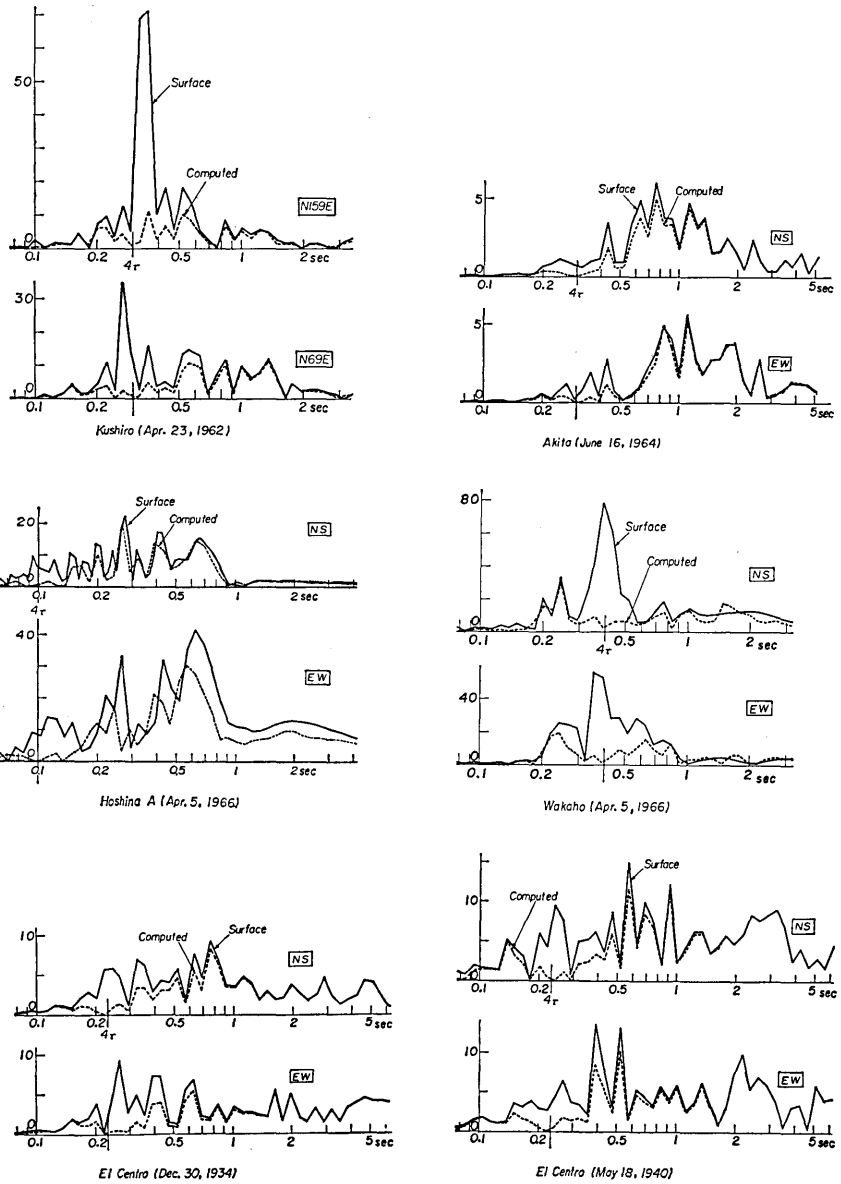

Fig. 11-a. Fourier spectra for observed and computed waveforms.

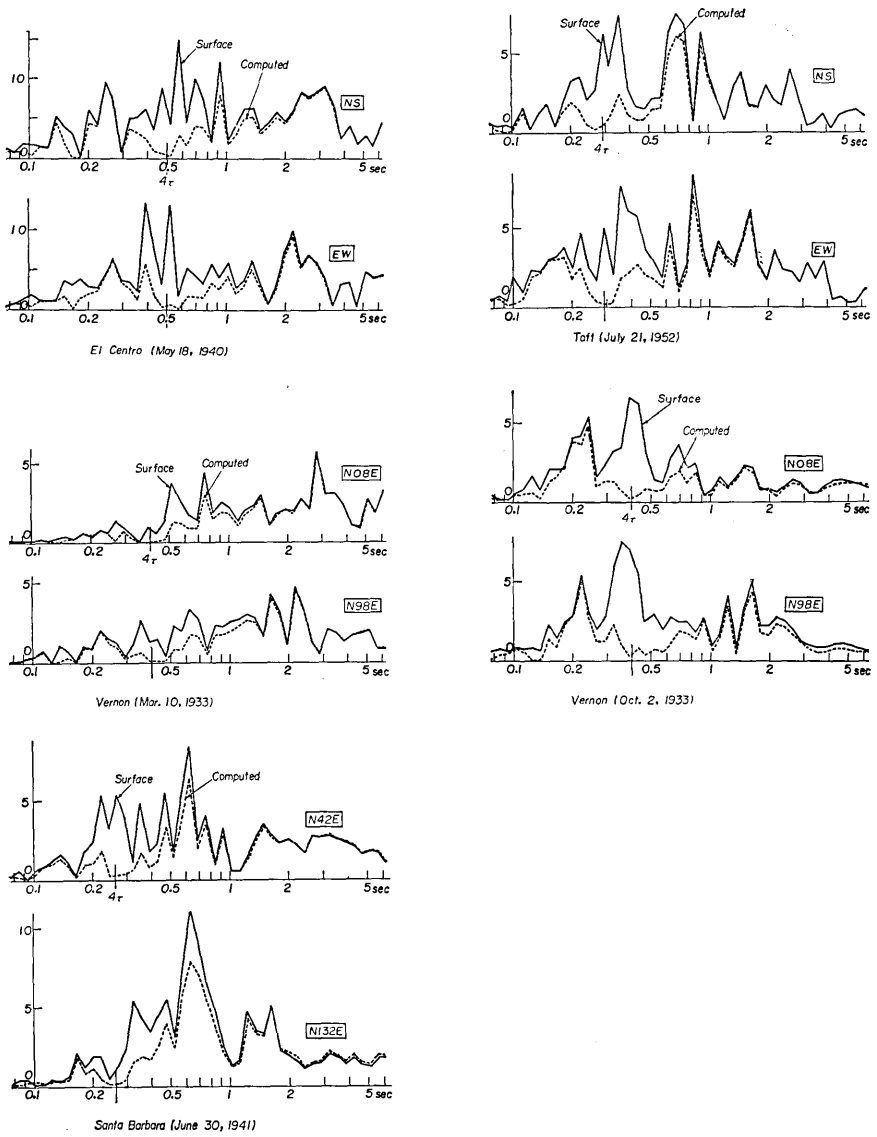

Fig. 11-b. Fourier spectra for observed and computed waveforms.

30. 構造物基礎基盤における強震波形について

地震研究所 吉沢静代・田中貞二・金井清

構造物の多質点モデルにたいする応答解析などに，日本やアメリカ合衆国で観測された強震記録が使われているが，これらの記録は，主として地表面付近で観測されたものである．

一方，重要構造物の基礎は，一般に，地表面にはなく，硬い地層までおりているから，この基礎基盤とでも云うべきところの地震波形を使う方が，地表面における強震波形をそのまゝ使うよりも合理的であると思われる．このため，地中における強震波形が得られていない現状では，地表での観測記録から，構造物の基礎基盤付近の地震動波形を推定することが考えられる．

日本およびアメリカ合衆国で得られたいくつかの強震記録について，このような試みを行ない，観測波形および得られた計算波形について，一質点系の応答スペクトルの形で，両者の比較を行なった．

その結果，両者の波形の構造物に与える影響はかなり違うことがわかった．